



Study of the electrical activation of Si + -implanted InGaAs by means of Raman scattering

S. Hernández, R. Cuscó, N. Blanco, G. González-Daz, and L. Artús

Citation: [Journal of Applied Physics](#) **93**, 2659 (2003); doi: 10.1063/1.1542659

View online: <http://dx.doi.org/10.1063/1.1542659>

View Table of Contents: <http://scitation.aip.org/content/aip/journal/jap/93/5?ver=pdfcov>

Published by the [AIP Publishing](#)



Re-register for Table of Content Alerts

Create a profile.



Sign up today!



Study of the electrical activation of Si⁺-implanted InGaAs by means of Raman scattering

S. Hernández and R. Cuscó

Institut Jaume Almera, Consell Superior d'Investigacions Científiques (CSIC), Lluís Solé i Sabarís s.n., 08028 Barcelona, Spain

N. Blanco and G. González-Díaz

Departamento de Electricidad y Electrónica, Facultad de Física, Universidad Complutense, 28040 Madrid, Spain

L. Artús^{a)}

Institut Jaume Almera, Consell Superior d'Investigacions Científiques (CSIC), Lluís Solé i Sabarís s.n., 08028 Barcelona, Spain

(Received 14 October 2002; accepted 4 December 2002)

Raman scattering has been used to study the lattice recovery and electrical activation of Si⁺-implanted In_{0.53}Ga_{0.47}As achieved by rapid thermal annealing. The degree of crystallinity recovery of totally amorphized samples is studied for annealing temperatures between 300 and 875 °C. A good degree of recovery is achieved for an annealing temperature of 600 °C. Higher annealing temperatures are required to electrically activate the Si donors. The observed LO phonon-plasmon coupled modes allow us to monitor the electrical activation by means of Raman scattering. We find that electrical activation sets in for annealing temperatures around 700 °C, and gradually increases up to an annealing temperature of 875 °C. The optimal conditions for the rapid thermal annealing are found to be 875 °C for 10 s. © 2003 American Institute of Physics.
[DOI: 10.1063/1.1542659]

I. INTRODUCTION

The InGaAs ternary alloy lattice matched to InP is a basic material for the fabrication of integrated optoelectronic circuits for high-speed fiber optic communications operating in the low-loss, low-dispersion window of optical fibers between 1.2 and 1.6 μm.^{1,2} High electron mobility and peak drift velocity make InGaAs also attractive for applications in high-speed field-effect transistors and microwave devices.^{3,4} A controlled selective area doping of InGaAs layers is required to fully exploit this material potential, and ion beam implantation has emerged as a versatile doping technique to realize the complex doping profiles required for device fabrication. Monolithic planar integration of a high-performance photodiode–junction-field-effect transistor combination has been achieved by using local Si- and Be-ion beam implantations to fabricate a junction field effect transistor on an optimized InGaAs/InP photodiode layer.⁵ Since ion beam implantation significantly damages the InGaAs crystal lattice,⁶ postimplantation annealing treatments are necessary to recover the host lattice and activate the dopants. Raman scattering has proved to be a sensitive tool to characterize the degree of lattice recovery after thermal annealing treatments, and Raman scattering criteria for anneal-restored zinc blende single crystals have been discussed in detail.⁷ Despite the technological importance of ion beam implantation in In_{0.53}Ga_{0.47}As, Raman scattering data on lattice recovery of implanted In_{0.53}Ga_{0.47}As are very scarce. In fact, only a Raman scattering study of the different degree of disorder in-

roduced in Ga–As and In–As bonds and their recovery upon furnace annealing has been reported on an In_{0.53}Ga_{0.47}As sample that was not fully amorphized by the implantation.⁸ However, current technological processing usually involves higher implantation doses and rapid thermal annealing (RTA) at higher temperatures than those reported in Ref. 8, and therefore a detailed Raman scattering analysis of implanted and annealed In_{0.53}Ga_{0.47}As is of great interest as a nondestructive characterization tool for ion-beam implantation processes in this material.

In this article, we present a Raman-scattering study of the lattice recovery and the electrical activation of In_{0.53}Ga_{0.47}As samples that were Si⁺ implanted to a high dose and subsequently annealed using RTA for a wide range of annealing temperatures. Raman spectra provide precise information not only about the gradual recovery of long range order in the crystal lattice with increasing annealing temperature, but also about the electrical activation of the dopants, and thus allows us to determine the optimum RTA conditions to achieve the best lattice recovery and highest dopant activation in the implanted In_{0.53}Ga_{0.47}As layers. The free-electron density can be estimated from the frequency of the Raman peaks associated with the LO-phonon–plasmon coupled modes that can be observed in the Raman spectra of the activated samples.

II. EXPERIMENT

In this work we have used (100)-oriented In_{0.53}Ga_{0.47}As wafers grown by the liquid-phase epitaxy (LPE) method on InP substrates. The samples were Si⁺ implanted at 150 keV

^{a)}Electronic mail: lartus@ija.csic.es

with a dose of $5 \times 10^{14} \text{ cm}^{-2}$. For these implantation conditions, TRIM calculations yield a peak Si concentration of $2.3 \times 10^{19} \text{ cm}^{-3}$ at 148 nm, with a longitudinal straggling of 87 nm. The implantations were performed with the samples tilted 7° off the (100) direction to minimize channeling effects. Postimplantation rapid thermal annealing cycles were carried out at 300, 400, 500, 600, 700, 800, 850, and 875 °C for 10 s in an MPT-600 reactor, using a graphite susceptor with the samples sandwiched between protective Si wafers in the so-called proximity geometry. The electrical activation of the samples was determined by Hall effect measurements on cross-pattern etched samples using the van der Pauw method taking the Hall factor as unity.

The Raman measurements were recorded at room temperature, using a T64000 Jobin–Ivon spectrometer equipped with a charge-coupled device (CCD) detector cooled with liquid nitrogen. Given the high optical absorption of $\text{In}_{0.53}\text{Ga}_{0.47}\text{As}$ in the visible,⁹ we used the 528.7 nm line of an Ar^+ laser as excitation source because this line gives the largest probing depth among the Ar^+ laser lines. From the data in Ref. 9, we obtain a Raman probing depth $z_R = 1/2\alpha$ of about 27 nm for the 528.7 nm line. The power on the samples was kept at $\approx 35 \text{ mW}$ to avoid heating and photoexcitation effects. To suppress the low-frequency Raman lines associated with interactions with atmospheric molecules, the low frequency Raman spectra were recorded with the samples under vacuum inside an optical cryostat. All the spectra were obtained on backscattering configuration from a (001) face.

III. RESULTS AND DISCUSSION

Figure 1 shows the room temperature Raman spectra of Si^+ -implanted $\text{In}_{0.53}\text{Ga}_{0.47}\text{As}$ samples annealed at increasing temperatures (B–I) compared with the spectrum of the as-grown material (A). The spectra were obtained in the $z(x'x')\bar{z}$ configuration, where $z \parallel [001]$ and $x' \parallel [110]$. In this configuration, Raman scattering by LO modes is allowed whereas TO modes are symmetry forbidden. $\text{In}_{1-x}\text{Ga}_x\text{As}$ is a two-mode behavior alloy that exhibits a strong GaAs-like LO intensity over the whole compositional range due to the coupling between the GaAs- and InAs-like oscillators.¹⁰ The spectrum of the as-grown sample [Fig. 1(A)] is dominated by an intense GaAs-like LO peak at 269.5 cm^{-1} , which confirms the nominal composition $x=0.47$ of the ternary alloy.¹⁰ The lowest frequency peak in the optical phonon region ($200\text{--}300 \text{ cm}^{-1}$) that is observed at 232 cm^{-1} is due to the InAs-like LO mode, whereas the peak that can be seen at $\approx 244 \text{ cm}^{-1}$ has been identified as an intrinsic disorder-activated mode of the alloy.^{11,12} Disorder-activated modes also give rise to Raman scattering bands in the acoustic phonon region ($40\text{--}200 \text{ cm}^{-1}$). The broad band detected between 100 and 190 cm^{-1} contains contributions from the disorder-activated longitudinal acoustic modes (DALA) as well as from the second-order transverse acoustic (2TA) modes of the $\text{In}_{0.53}\text{Ga}_{0.47}\text{As}$ lattice, whereas the weaker band centered at $\approx 60 \text{ cm}^{-1}$ is due to disorder-activated transverse acoustic (DATA) modes.¹³ Second-order optical modes, shown in the inset of Fig. 1, although being notably softened

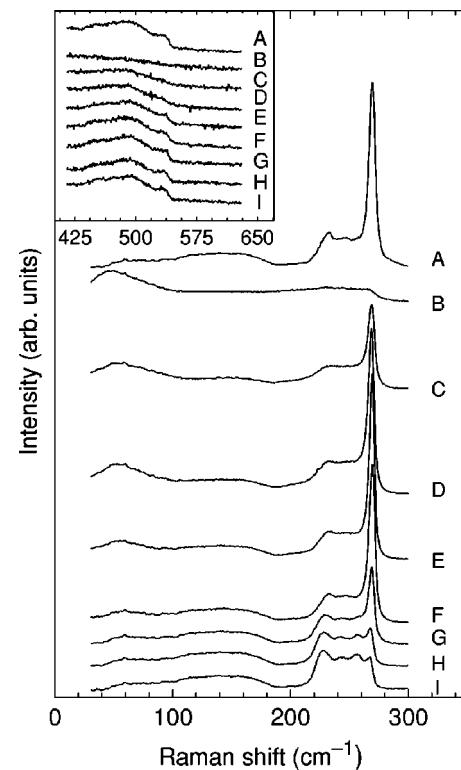


FIG. 1. Room temperature $z(x'x')\bar{z}$ Raman spectra of $\text{In}_{0.53}\text{Ga}_{0.47}\text{As}$ samples that were Si^+ implanted to $5 \times 10^{14} \text{ cm}^{-2}$ Si^+ and annealed at 300 (C), 400 (D), 500 (E), 600 (F), 700 (G), 800 (H), and 875 °C (I), compared with the spectrum of virgin $\text{In}_{0.53}\text{Ga}_{0.47}\text{As}$ (A) and that of the implanted sample before RTA (B).

by the alloying, display a characteristic feature at $\approx 539 \text{ cm}^{-1}$ corresponding to the GaAs-like 2LO mode scattering.

Si^+ implantation at 150 keV to $5 \times 10^{14} \text{ cm}^{-2}$ in $\text{In}_{0.53}\text{Ga}_{0.47}\text{As}$ results in the formation of a fully amorphized layer,⁶ which is confirmed by the featureless Raman spectrum of the implanted $\text{In}_{0.53}\text{Ga}_{0.47}\text{As}$ sample prior to RTA shown in Fig. 1(B). As can be seen from the spectrum in Fig. 1(C) displaying a well-defined GaAs-like LO Raman peak, even a low temperature RTA at 300 °C yields a noticeable lattice recovery of the implanted sample. However, a large degree of disorder still remains in this sample, as indicated by the prominent DATA band observed between 30 and 80 cm^{-1} and the featureless second-order optical spectrum (inset). The intensity of the band between 100 and 190 cm^{-1} , which as discussed above arises from scattering by DALA and 2TA modes, is weaker than in the as-grown sample. This indicates that 2TA scattering, which is strongly reduced by the presence of disorder, has a substantial contribution to this band in virgin $\text{In}_{0.53}\text{Ga}_{0.47}\text{As}$, whereas the band observed in spectrum C is mainly due to DALA modes. The GaAs-like LO peak of the sample annealed at 300 °C displays larger width and more marked low-frequency asymmetry than the as-grown sample, which is associated with the activation of $q \neq 0$ modes by the implantation-induced disorder.

With increasing annealing temperature up to 600 °C, the Raman spectra [Figs. 1(D)–1(F)] show a gradual intensity

increase and sharpening of the optical modes, together with an intensity reduction of the low-frequency DATA band. In the spectrum of the sample annealed at 600 °C [Fig. 1(F)] both the GaAs- and InAs-like LO peaks display intensities similar to those of the virgin $\text{In}_{0.53}\text{Ga}_{0.47}\text{As}$ sample. In this sample, the second-order optical band and a distinct 2LO feature is clearly detected, and the 2TA band resembles that observed in the virgin sample whereas the DATA band is very weak. Therefore, we conclude that an excellent lattice recovery is already achieved by RTA at 600 °C for 10 s.

When the annealing temperature is increased to 700 °C the only noticeable effect on the Raman spectrum [Fig. 1(G)] is an intensity reduction of the GaAs-like LO peak, which signals the onset of electrical activation of the implanted impurities. In fact, when electrical activation occurs, the resulting free electron gas couples with the polar longitudinal modes of the lattice and, consequently, the unscreened LO modes observed in the Raman spectra arise only from the surface depletion region. The relatively high intensity of the GaAs-like LO mode in spectrum G indicates a sizable extension of the depletion region and hence a low electron concentration.

With a further increase of the annealing temperature, the optical phonon region changes noticeably [see Figs. 1(H) and 1(I)], displaying four Raman peaks instead of the three peaks typically observed in the $\text{In}_{0.53}\text{Ga}_{0.47}\text{As}$ Raman spectrum. These changes in the Raman spectrum reflect the increasing electrical activation of the implanted dopants. In fact, the additional peak that emerges at 257 cm^{-1} in spectra H and I corresponds to the intermediate-frequency coupled mode (IFCM) arising from LO phonon-plasmon coupling in ternary alloys.¹⁴ Furthermore, we note that in spectra H and I the lowest frequency peak in the optical region is found at about 228 cm^{-1} , a frequency lower than the InAs-like LO mode of the $\text{In}_{0.53}\text{Ga}_{0.47}\text{As}$ alloy that is observed in spectra A and C to F. This peak is due to the low-frequency coupled mode (LFCM) of the ternary alloy,¹⁴ which overlaps the InAs-like LO mode.

The Raman spectra displayed in Fig. 1 show that while the crystallinity of the implanted $\text{In}_{0.53}\text{Ga}_{0.47}\text{As}$ layer is practically recovered by RTA at 600 °C, higher annealing temperatures are required to electrically activate the dopants. The frequency of the L_+ coupled mode, being highly sensitive to changes in the free electron concentration, can be used to assess the electrical activation achieved by RTA under different conditions. Figure 2 shows the Raman spectra of implanted $\text{In}_{0.53}\text{Ga}_{0.47}\text{As}$ samples after RTA at 800, 850, and 875 °C. A broad Raman scattering band can be observed in the region between 650 and 1050 cm^{-1} corresponding to the L_+ coupled modes. The intensity of the L_+ band is very weak for the sample annealed at 800 °C (spectrum A). This correlates well with the sizable intensity of the depletion-region LO mode, indicating that the density of free electrons is low enough to give rise to a surface depletion width that is a substantial fraction of the laser probing depth. As can be seen in Fig. 2(B), a small increase of the annealing temperature up to 850 °C results in a strong intensity reduction of the depletion-region LO mode accompanied by an intensity increase and a shift to higher frequencies of the L_+ modes.

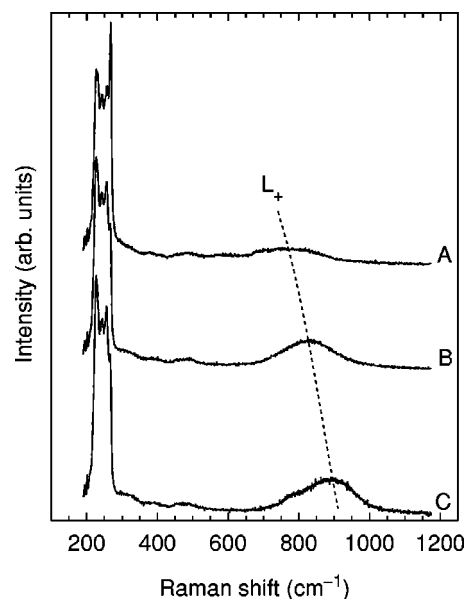


FIG. 2. Room temperature $z(xy)z$ Raman spectra of Si^+ -implanted $\text{In}_{0.53}\text{Ga}_{0.47}\text{As}$ samples subsequently annealed at 800 (A), 850 (B), and 875 °C (C). The dashed line is a guide to the eye.

Although a further increase of annealing temperature up to 875 °C has no noticeable effect on the depletion-region LO peak intensity, the L_+ still shows a remarkable upward shift that reflects the free electron density increase achieved with this annealing temperature.

The high sensitivity to the free-electron density of the L_+ mode in $\text{In}_{0.53}\text{Ga}_{0.47}\text{As}$ can be advantageously used to characterize the electrical activation of implanted and annealed samples. In bulk doped $\text{In}_{0.53}\text{Ga}_{0.47}\text{As}$, we have shown that the free-electron density that can be obtained from L_+ line-shape fits to the Raman spectra is in very good agreement with Hall effect determinations when the Lindhard–Mermin model is used.¹⁴ This model, which takes explicitly into account the wave-vector dependence of the modes, the conduction band nonparabolicity, and Landau-damping effects, must be used to obtain a reliable description of the coupled-mode behavior in $\text{In}_{0.53}\text{Ga}_{0.47}\text{As}$ because of the low values of the electron effective mass and of the optical-phonon frequencies in this alloy. In Fig. 3 we plot the dependence of the coupled mode energies on the electron density for $\text{In}_{0.53}\text{Ga}_{0.47}\text{As}$ at room temperature calculated with the Lindhard–Mermin model for an electronic damping of 40 cm^{-1} , which was typically observed for this range of electron densities in $n\text{-In}_{0.53}\text{Ga}_{0.47}\text{As}$ samples.¹⁴ The wave-vector uncertainty associated with the high optical absorption of the $\text{In}_{0.53}\text{Ga}_{0.47}\text{As}$ alloy for the exciting wavelength has been taken into account in the calculations. In contrast with the LFCMs and the IFCMs, which are well into the Landau damping regime and asymptotically approach the TO modes of the alloy,¹⁴ the L_+ mode exhibits a high sensitivity to the electron density, increasing its frequency by 500 cm^{-1} between electron densities of 10^{18} and 10^{19} cm^{-3} . The L_+ bands observed in the implanted $\text{In}_{0.53}\text{Ga}_{0.47}\text{As}$ layers are much broader than those observed in epitaxially doped $\text{In}_{0.53}\text{Ga}_{0.47}\text{As}$ crystals.¹⁴ This is a consequence of the inho-

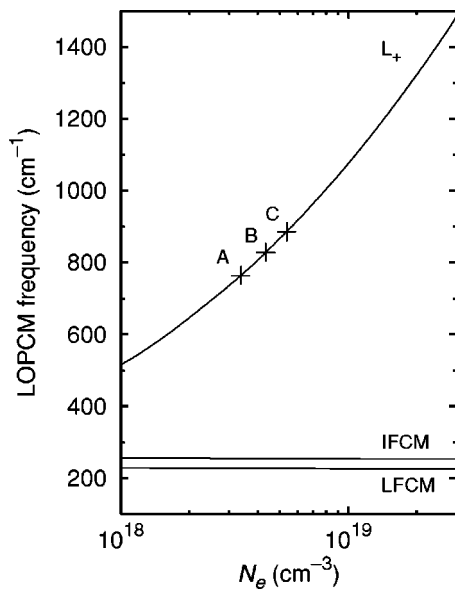


FIG. 3. Room temperature $\text{In}_{0.53}\text{Ga}_{0.47}\text{As}$ coupled-mode dispersion curves calculated using the Lindhard–Mermin model and taking into account absorption effects. The crosses indicate the L_+ frequencies observed in the Raman spectra of the samples annealed at 800 (A), 850 (B), and 875 °C (C).

mogenous doping profile produced by the ion beam implantation. Given the high optical absorption of $\text{In}_{0.53}\text{Ga}_{0.47}\text{As}$ for the excitation wavelength used ($\alpha = 1.83 \times 10^5 \text{ cm}^{-1}$),⁹ Raman scattering measurements probe only a region of the doping profile near the surface. According to the calculated L_+ dispersion of Fig. 3 and using the L_+ frequencies obtained from the spectra shown in Fig. 2, we obtain electron densities of 3.4×10^{18} , 4.3×10^{18} , and $5.4 \times 10^{18} \text{ cm}^{-3}$ for the samples annealed at (A) 800, (B) 850, and (C) 875 °C, respectively. It should be emphasized that relatively small changes of annealing temperature in this range yield significantly different values of the electron density in the implanted samples, which can be accurately monitored by means of Raman scattering measurements.

The electrical activations obtained for these samples from Hall effect measurements were, respectively, (A) 35%, (B) 43%, and (C) 59%. From these activation values, and assuming the doping profile given by TRIM calculations, we estimate that the electron density values at the Raman probing depth ($z_R = 1/2\alpha$) are (A) 3.2×10^{18} , (B) 3.9×10^{18} , and (C) $5.4 \times 10^{18} \text{ cm}^{-3}$. These are in good agreement with the values obtained above from the L_+ mode frequency observed in the Raman spectra, which confirms that Raman scattering can be used as a sensitive, nondestructive tool to monitor the electrical activation of implanted samples provided that a suitable line-shape model is used and the finite penetration of the laser line is taken into account. From the Raman scattering results shown in Figs. 2 and 3 we conclude

that RTA at 875 °C for 10 s achieves a very good lattice recovery and yields the highest electrical activation in Si^+ -implanted $\text{In}_{0.53}\text{Ga}_{0.47}\text{As}$ layers. Higher annealing temperatures have been shown to lead to sample degradation due to phosphorus diffusion and stoichiometry alterations.^{15,16}

IV. CONCLUSIONS

We have carried out a Raman scattering study of the lattice recovery by RTA on Si^+ -implanted $\text{In}_{0.53}\text{Ga}_{0.47}\text{As}$. We find that an excellent lattice recovery is already achieved for an annealing temperature of 600 °C, although higher annealing temperatures are required to electrically activate the Si impurities. Raman scattering provides a nondestructive and very sensitive tool to assess both the lattice recovery and the onset of electrical activation as the annealing temperature is increased. The frequency of the L_+ coupled modes can be used to obtain an estimation of the electrical activation that is in very good agreement with the electrical activation determined by means of Hall effect measurements. According to the Raman scattering results, the optimal RTA conditions for Si^+ -implanted $\text{In}_{0.53}\text{Ga}_{0.47}\text{As}$ are found to be 875 °C for 10 s.

ACKNOWLEDGMENTS

The authors wish to acknowledge the Spanish Ministerio de Ciencia y Tecnología for financial support. One of the authors (S.H.) acknowledges support from the Departament d'Universitats i Recerca de la Generalitat de Catalunya.

- ¹Y. G. Wey, D. L. Crawford, K. Giboney, J. E. Bowers, M. J. Rodwell, P. Silvestre, M. J. Hafich, and G. Y. Robinson, *Appl. Phys. Lett.* **58**, 2156 (1991).
- ²F. E. Ejeckam, C. L. Chua, Z. H. Zhu, Y. H. Lo, M. Hong, and R. Bhat, *Appl. Phys. Lett.* **67**, 3936 (1995).
- ³K. W. Wang, C. L. Cheng, J. Long, and D. Mitcham, *IEEE Electron Device Lett.* **9**, 205 (1988).
- ⁴S. Koumetz, J. Marcon, K. Ketata, M. Ketata, C. Dubon-Chevalier, P. Launay, and J. L. Benchimol, *Appl. Phys. Lett.* **67**, 2161 (1995).
- ⁵J. G. Bauer, H. Albrecht, L. Hoffmann, D. Römer, and J. W. Walter, *IEEE Photonics Technol. Lett.* **8**, 566 (1996).
- ⁶S. Hernández, B. Marcos, R. Cuscó, N. Blanco, G. González-Díaz, and L. Artús, *J. Lumin.* **87-89**, 721 (2000).
- ⁷L. Artús, R. Cuscó, J. Ibáñez, J. M. Martín, and G. González-Díaz, *J. Appl. Phys.* **82**, 3736 (1997).
- ⁸K. Kamimoto and T. Katoda, *Appl. Phys. Lett.* **42**, 811 (1983).
- ⁹S. M. Kelso, D. E. Aspnes, M. A. Pollack, and R. E. Nahory, *Phys. Rev. B* **26**, 6669 (1982).
- ¹⁰J. Groenen, R. Carles, G. Landa, C. Guerret-Piécourt, C. Fontaine, and M. Gendry, *Phys. Rev. B* **58**, 10 452 (1998).
- ¹¹T. P. Pearsall, R. Carles, and J. C. Portal, *Appl. Phys. Lett.* **42**, 436 (1983).
- ¹²J. P. Estrera, P. D. Stevens, R. Glosser, W. M. Duncan, Y. C. Kao, H. Y. Liu, and E. A. Beam III, *Appl. Phys. Lett.* **61**, 1927 (1992).
- ¹³G. Landa, R. Carles, and J. B. Renucci, *Solid State Commun.* **86**, 351 (1993).
- ¹⁴R. Cuscó, L. Artús, S. Hernández, J. Ibáñez, and M. Hopkinson, *Phys. Rev. B* **65**, 35210 (2002).
- ¹⁵M. N. Blanco, E. Redondo, F. Calle, I. Mártel, and G. González-Díaz, *J. Appl. Phys.* **87**, 3478 (2000).
- ¹⁶S. Hernández, N. Blanco, I. Mártel, G. González-Díaz, R. Cuscó, and L. Artús, to appear in *J. Appl. Phys.* (2003).